Characterization of the Weak Link of Wool Fibers

Weidong Yu,[1] Ron Postle,[2] Haojing Yan[1]

[1]*College of Textiles, Donghua University, 1882 West Yan-An Road, Shanghai 200051, People's Republic of China*
[2]*Department of Textile Technology, University of New South Wales, Sydney 2052, Australia*

Received 14 August 2001; accepted 17 December 2002

ABSTRACT: The variance of fiber morphology along a fiber and the natural and artificial flaws in the fiber structure represent the primary reasons for the weak link of fibers. Accordingly, the fiber weak link can be divided into two types, that is, the geometrical thinnest part and the structural weak point. Scanning electron microscopic observation was used to characterize the morphological features of the fiber weak points whose forms are the normal thin sections, natural flaws, and artificial damage. Both the fiber profile morphology and the tensile behavior of wool fibers have been measured using a single-fiber analyzer (SIFAN) and an optical microscope with a CCD camera plus an XQ-1 fiber tensile tester (OM + XQ). The results from the SIFAN and OM+XQ methods indicate that the fibers breaking at their minimum diameters represent only one part of the broken fibers. The percentage of this kind of breakage is in the range of 40–60%. A new approach is presented to identify the weak-point breakage relying on the fiber tensile behavior. The experimental results show that the probabilities of weak-point, normal, and thinnest-part breakage evaluated by these methods approximate 40, 60, and slightly more than 80%, respectively. © 2003 Wiley Periodicals, Inc. J Appl Polym Sci 90: 1206–1212, 2003

INTRODUCTION

It is well known that the wool diameter is not uniform between fibers and along the length of individual fibers. Regarding the difference between fibers, there are many methods for the measurement of the fiber diameter but four methods are the most important for standard testing purposes, that is, using an optical projection microscope (OM),[1] an arealometer,[2] optical fiber diameter analysis (OFDA),[3,4] and a SIRO–laser-scan fiber diameter instrument (LaserScan).[5]

For the diameter variance along a fiber, a few methods, such as the single-fiber analyzer (SIFAN)[6,7] and OFDA,[8,9] could be used efficiently to measure the diameter variance parameter (and the tensile behavior of the fiber *in situ* for SIFAN only). The thinnest section would usually be regarded as the weaklink of the fiber, to result in a relatively poor-quality wool. Generally, the thinnest position measured by SIFAN is the weakest part of a fiber only if the structure is a homogeneous structure along the fiber. If the fiber structure is inhomogeneous, the weaklink at a relatively thick part, or even at the thinnest part, is difficult to determine.

Some research has been done on fiber breakage at its thin sections. The results from Anderson and Cox[10] showed that a significantly higher correlation existed between the fiber strength and the mean fiber diameter than that between the strength and the observed diameter nearest to the broken point. Although they did not give any clear explanation, the probable reason is that the diameter in their measurement is far from the real breaking point because it is impossible to detect the real minimum diameter by measuring only five points on a 1.5-cm fiber length. Conversely, Woods et al.[11] reported that a high positive correlation between the fiber strength and the cross-sectional area at break for wool was found by experimental analysis.

In practice, the explanation that fiber breakage occurs at the thinnest part of a fiber is not universally accepted. The alternative approach is to find and identify the intrinsic structural reason for a fiber breaking at its weak spot. The early work of the fiber cross section of tender wool observed by SEM was done by Hunter et al.[12]; Zimmermann and Hocker[13] investigated the fiber broken ends and measured the bundle tensile properties of the wool; Orwin et al.[14,15] examined the broken region of both tender and sound wools from Romney sheep; and Thorsen[16] also reported these findings in his work.

Some more elaborate investigations have been performed on the following aspects: Hepworth et al.[17] designed a tensile stage used in SEM and observed the tensile fracture of Lincoln wool. Hearle et al.[18] observed the fracture features of keratin fibers under various environmental conditions and indicated that the morphology of the broken ends was related to the fiber cortical structure and testing conditions. Bandyopadhyay[19] and Yang et al.[20] used a tensile stage to

Correspondence to: W. Yu.

Journal of Applied Polymer Science, Vol. 90, 1206–1212 (2003)

study the deformation of wool fibers in extension and recognized that a crack developed in the cuticular cell until the cortical cells were exposed and then the cuticle slides over the cortex after the breakdown of the intercellular cement between the cortex cells. Gharehaghaji et al.[21,22] reported their research on the effects of wool fiber microdamage caused by the opening textile processes on tensile failure and compressive microdamage, using scanning electron microscopy (SEM).

Although Peirce[23] set forth the principle of the weak link in 1926, few subsequent reports have considered the difference between the fiber's thinnest parts and the structural weak points. The effect on the fiber-breaking properties of different types of weak link has not been determined, especially the weak point of the fiber with an inhomogeneous structure.

Accordingly, the characteristics of the weak points in a wool fiber are observed and discussed in the present article. A new approach is proposed to identify these weak links.

EXPERIMENTAL

SIFAN methods

The profile and tensile properties of two kinds of wool fiber which are SH80s and 26 μm collected from the Shanghai Wool Top-Making Mill (Shanghai, China), were measured automatically by the SIFAN instrument[6] under standard conditions (20 ± 2°C; 65 ± 3% RH). The SIFAN was used in the present study to measure each projected width along a fiber at 40-μm intervals, so it supplies the average diameter D_{ave} of a fiber and the fiber-diameter deviation not only between fibers, CVD, but also along a single fiber, CVD_{ave}.

It should be mentioned that SIFAN has one particular defect in measuring, although it has many advantages. There are blind angles at the two clamped fiber ends according to Figure 1, because the light beam used to detect the fiber's projected width is inclined but not perpendicular to the fiber axis. The blind angle θ will result in an undetectable area (L_θ) about 5 mm

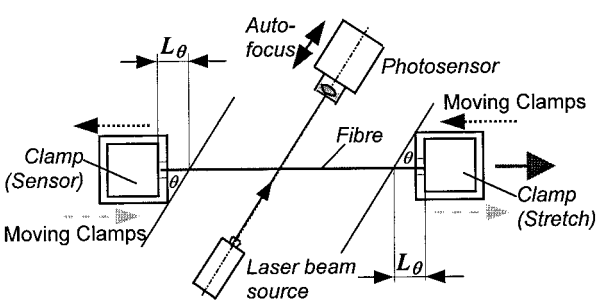

Figure 1 Diagram showing the principle of measurement of the SIFAN instrument.

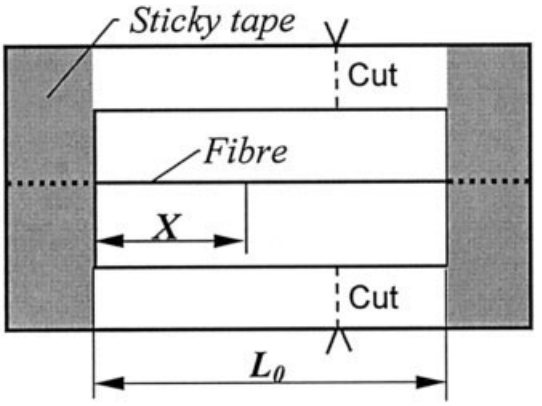

Figure 2 Schematic diagram of the paper window fiber sample for OM+XQ methods.

long at each fiber end, that is, there is nearly a 10 mm length of fiber undetected for each individual fiber. If, therefore, a short gauge length is chosen, there would exist a high possibility of failure to detect the minimum diameter point. In general, SIFAN should be used for relatively long-gauge-length fiber testing. The gauge length was 50 mm long in the present experiment.

Optical projection microscope (OM) and fiber tensile test (XQ) methods

The two wool fiber samples were also tested under the same conditions as above using the OM + XQ method, that is, an optical microscope with a CCD camera plus the XQ-1 fiber tensile tester developed by the China Textile University.[24]

The method involved sticking a straightened fiber over a paper window with a gauge length, L_θ, as shown in Figure 2. The thinnest part of the fiber was then observed by using OM to record the projected width D_{min} and its position X_{Dmin}. Finally, the paper window was cut and the fiber was stretched for the tensile measurement.

Both methods measure, first, D_{min} and $X_{D_{min}}$ of a single fiber. Then, the tensile properties of the single fiber are tested. Last, the real breaking position X_{break} is recorded. These experiments, as well as SEM observations, led to some meaningful and interesting results and discussions on the fiber's geometrical characteristics and the tensile properties at the fiber's weak points.

RESULTS AND DISCUSSION

Profile along the fiber length

The fiber diameter measured by SIFAN represents the thickness at different positions along the fiber length. The typical profile curves of fine and thick wool fibers are shown in Figure 3(a). The lowest point is the

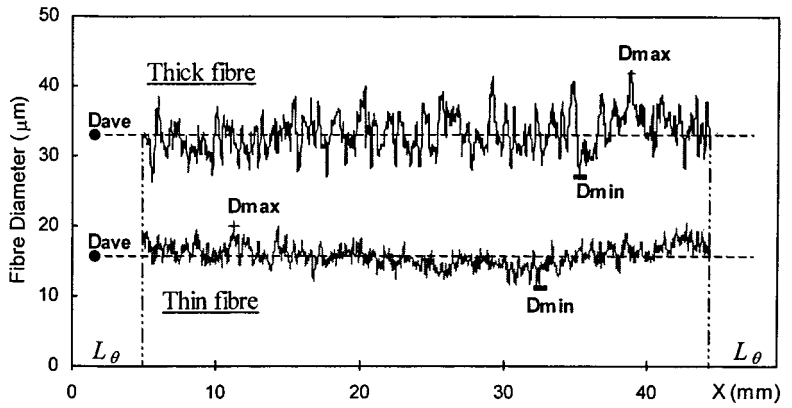

(a) Normal profiles of thin and thick wool fibres

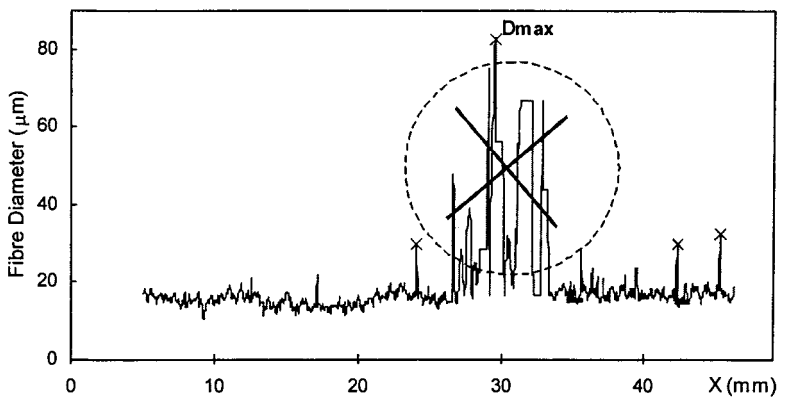

(b) The fibre profile affected by dust and other non-fibrous attachments

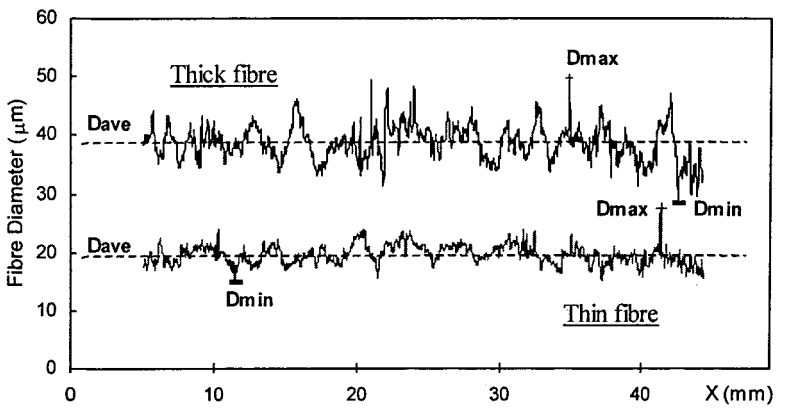

(c) Fibre profiles with significant waves caused by crimp and twist

Figure 3 Fiber profile curves along the fiber length measured by SIFAN.

minimum diameter, D_{min}, and the highest peak is the maximum diameter, D_{max}.

It is evident that the following factors influence the accuracy of D_{min} and D_{min}:

(i) The actual detecting-length, that is, $L_0 - 2L_\theta$, because the geometric probability to find D_{min} and D_{max} is equal to $(L_0 - 2L_\theta)/L_0$ ($\approx (L_0 - 10)/L_0$, where L_0 is the gauge length, and L_θ, the undetected length (see Fig. 1);

(ii) The interval between the detecting points, because a long interval would result in a decrease of the accuracy in the measurement of D_{min} and D_{max};

(iii) Fiber noncircularity;

(iv) Abnormal pulse signals in the fiber profile curves by reason of nonfibrous attachments, as shown in Figure 3(b); and

(v) The difficulty to focus on a fiber during dynamic measurement due to fiber crimp and

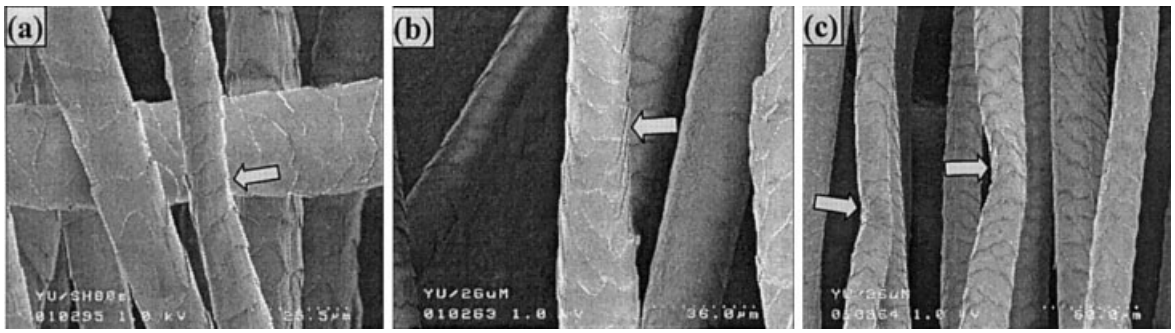

Figure 4 SEM photographs for the thin parts of wool fibers, thinning (a) gradually, (b) at a medium rate, and (c) sharply.

twist or due to the dark and bright parts on the fiber, [see the wave curves in Fig. 3(c)].

The measures which could be taken to reduce or to avoid the influence caused by the above factors are as follows:

(i) To adopt a longer gauge length, that is, >50 mm, so that the probability to find D_{min} and D_{max} could be higher than 80%;
(ii) To adopt a reasonable detecting interval for the fiber profile scanning (the interval relates to the fiber diameter, i.e., 20–40 μm);
(iii) To turn the fiber to a certain angle (90°) and then to measure the fiber profile again (this method is not used in this present article);
(iv) To shorten the exposure time of the fiber samples as much as possible to avoid dust contamination; and
(v) To insert a higher pretension to remove fiber crimp and to avoid twisting the fibers.

Generally, the smaller D_{min} or D_{min}/D_{ave}, is the weaker are the fibers, especially so for the ratio D_{min}/D_{ave}. This is of particular interest because it is most important for wool processors to know the real quality of wool.

Geometric features of the fiber weak point

The fiber weak point is the essential cause of fiber breakage. As far as fiber morphology is concerned, the thinner parts and the morphological deformations of a fiber represent the two major forms of fiber weak points, called the geometric weak links. The former is the thinnest part of a fiber and the latter represents fiber flaws and damage.

The geometric characteristics of the fiber weak point were observed by SEM and exhibit three main forms, as shown in Figures 4–6. The "normal" thin parts (see Fig. 4) are not necessarily the true structural weak points because their appearance is relatively even, but the thin part (thinning sharply), as shown in Figure 4(c), is also probably a structural weak point. The natural flaws illustrated in Figure 5 and the artificial damage shown in Figure 6 both represent structural weak points which will inevitably result in the deterioration of the fiber tensile properties and fiber breakage at these positions, whether these sections are thick or thin.

Fiber breakage at the minimum fiber diameter D_{min}

According to the definitions of D_{min}, $X_{D_{min}}$, and X_{break}, two types of wool were tested by both SIFAN and OM

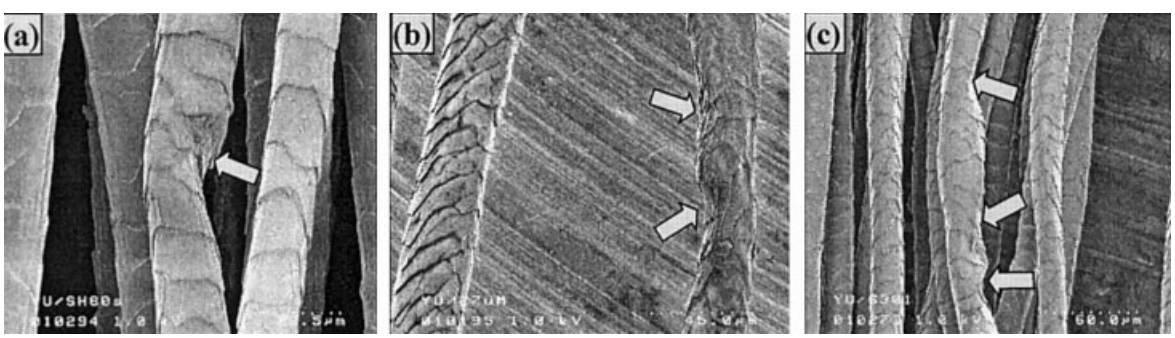

Figure 5 SEM photographs for the outer-structure natural flaws, of wool fibers, (a) sharp thin-neck; (b) weathering damage; (c) aberrant parts.

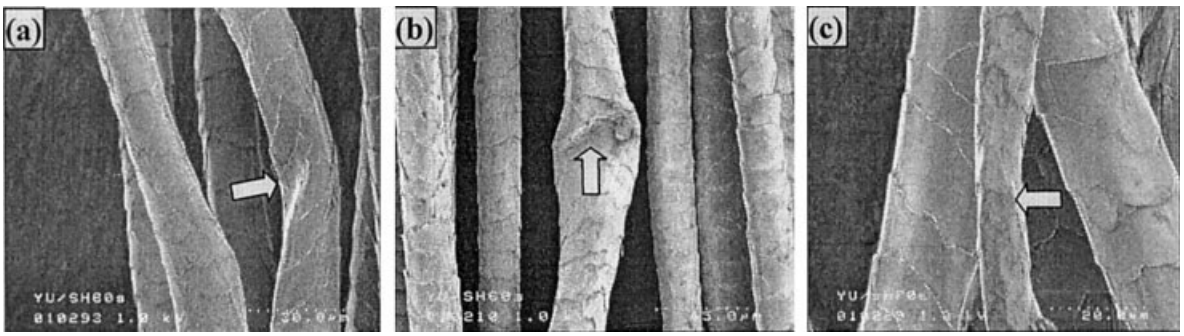

Figure 6 SEM photographs for the artificial damage of wool fibers; (a) bending and pressing; (b) ramming; (c) scraping and polishing.

+ XQ − 1. The number, $N_{D_{min}}$, and the percentage, $P_{D_{min}}$, of the fiber, breakage at D_{min}, that is $X_{brok} = X_{D_{min}}$, are evaluated in Table I. In fact, $P_{D_{min}}$ is not high, only about 40–60%, as shown in the last column of Table I. The other 40–60% fibers are probably broken at the true structural weak point or at the real thinnest part of the fiber located at the thick or noncircular cross sections, respectively.

These results indicate that the D_{min} measured by SIFAN is sometimes not the real minimum fiber diameter. The percentage of fibers breaking at D_{min} obtained from SIFAN is evidently lower than that obtained from the OM + XQ method. The reason relates mainly to the fact that there are undetected fiber sections at the two clamped ends in the SIFAN instrument.

Tensile characteristics of fiber weak points

During stretching, fiber breakage must occur at either the thinnest part or the true structural weak point. The broken parts of the fiber can be observed by OM or SEM, and $P_{D_{min}}$ can be found from the probability of the "normal" and weak-point breakage at the D_{min} of a fiber.

However, it is very difficult to affirm whether the fiber breaks according to the weak-point breakage or the "normal" breakage, where the normal breakage means that the fiber tensile curve is integrated, as illustrated in Figure 4, that is, fiber tenacity and extension are relatively large. In accordance with these characteristics, the two types of fiber breakage can be distinguished by the critical values of fiber stress and strain, σ_{cri} and ε_{cri}, respectively (see Fig. 7).

The identification steps are shown in Figure 8 and are described as follows:

(1) Find the number, $N_{D_{min}}$, of all fibers breaking at $X_{break} = X_{D_{min}}$, and to calculate its percentage, $P_{D_{min}} = 100N_{D_{min}}/N$, where N is the total fiber number (see Table I).
(2) Calculate the average stress $\bar{\sigma}_{D_{min}}$ or the average strain $\bar{\varepsilon}_{D_{min}}$ at D_{min}, then let $\sigma_{cri} \approx \bar{\sigma}_{D_{min}}$ and $\varepsilon_{cri} \approx \bar{\varepsilon}_{D_{min}}$ as a criterion for identification, that is:
   (i) If $\sigma \le \sigma_{cri}$ or $\varepsilon \le \varepsilon_{cri}$, the fiber is recognized as the weak-point breakage at D_{min} and its number and percentage are N_{WD} and P_{WD}, respectively;
   (ii) If $\sigma > \sigma_{cri}$ or $\varepsilon > \varepsilon_{cri}$, the fiber exhibits normal breakage at D_{min} and its number and percentage are N_{WD} and P_{WD}, respectively, as shown in the A/B flow diagram in Figure 8.

(3) Select all the fibers whose $X_{break} \neq X_{D_{min}}$ and calculate the percentage, $P_{UD} = 1 - P_{D_{min}}$.
(4) Identify the breaking form of the fibers from (3) by using σ_{cri} and ε_{cri} so
   (i) If $\sigma > \sigma_{cri}$ or $\varepsilon > \varepsilon_{cri}$, the fiber must be broken at the real thinnest part because the fiber is a homogeneous one in tensile behavior and the normal breakage should occur at the thinnest part, and, therefore, its

TABLE I
Numbers and Percentage of Fibers Breaking at D_{min}

Sample no.	Top name	Instrument	N (number)	$N_{D_{min}}$ ($X_{break} = X_{D_{min}}$)	$N_{Ud_{min}}$ [a] $X_{break} \neq X_{D_{min}}$	$P_{D_{min}}$ (%)
1	SH80s	OM + XQ	342	203	139	59.4
2	26 μm	OM + XQ	194	110	84	56.7
3	SH80s	SIFAN	254	123	131	48.4
4	26 μm	SIFAN	148	62	86	41.9

[a] $N_{Ud_{min}} = N - N_{D_{min}}$.

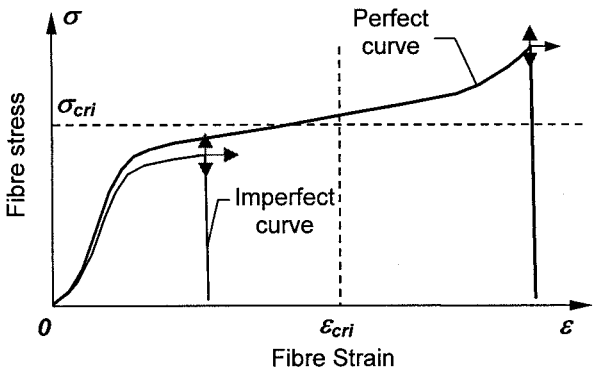

Figure 7 Schematic diagram of fiber stress–strain curves with different breaking behavior.

number and percentage are N_{NT} and P_{NT} (i.e., N_{NUD} and P_{NUD}), respectively; and

(ii) If $\sigma \leq \sigma_{cri}$ or $\varepsilon \leq \varepsilon_{cri}$, the fiber is recognized as the weak-point breakage but not at D_{min} and its number and percentage are N_{WUD} and P_{WUD}, respectively.

The case (4)–(ii) above is correct where $\varepsilon \leq \varepsilon_{cri}$. As for the situation where $\sigma \leq \sigma_{cri}$, there are not only the weak-point breakage fibers, but also the normal breakage fibers whose breaking points do not occur at D_{min}. Therefore, ε_{cri} is necessarily introduced for the further identification of the case of $\sigma \leq \sigma_{cri}$ (A′ sequence in Fig. 8), that is:

(i) If $\varepsilon \leq \varepsilon_{cri}$, the fibers are broken at the weak points and the fiber number and probability for the case are N_{WWUD} and P_{WWUD}, respectively; and

(ii) If $\varepsilon > \varepsilon_{cri}$, the breakage of fibers belongs to the normal breaking case at the real thinnest position and its number and percentage are N_{NWUD} and P_{NWUD}, respectively.

For stress identification, P^{σ}_{W} ($= P^{\sigma}_{WD} + P^{\sigma}_{WWUD}$) is the total percent of weak-point breakage; $P^{\sigma}_{N} = P^{\sigma}_{NT} + P^{\sigma}_{NWUD}$ is the normal-breakage percent, and P^{σ}_{Th} ($\approx P^{\sigma}_{Dmin} + P^{\sigma}_{NWUD} + P^{\sigma}_{NT}$) represents the percent of fiber breakage at the thinnest part because there also exists the probability of fiber breaking at the real thinnest part in P^{σ}_{WWUD}. In fact, $P^{\sigma}_{NWUD} + P^{\sigma}_{NT}$ is the probability of the D_{min} being misrepresented by SIFAN. For strain identification, $P^{\varepsilon}_{W} = P^{\varepsilon}_{WD} + P^{\varepsilon}_{WUD}$, $P^{\varepsilon}_{N} = P^{\varepsilon}_{ND} + P^{\varepsilon}_{NT}$, and $P^{\varepsilon}_{Th} = P^{\varepsilon}_{Dmin} + P^{\varepsilon}_{NT}$.

The experimental results of fiber-breaking features obtained by the OM + XQ and the SIFAN methods are listed in Table II for the wool sample SH80s. $\bar{T}_{D_{min}}$ and $\bar{\varepsilon}_{D_{min}}$, that is, the average tenacity and extension of the fibers broken at D_{min}, are used instead of the critical stress and strain, respectively. The results from the two methods are coincident and the probabilities of the weak-point and normal breakage are approximately 42 and 58%, respectively. The percentage of fiber breakage at the thinnest part is 82.3–85.4% based on $\bar{T}_{D_{min}}$ or 81% determined by $\bar{\varepsilon}_{D_{min}}$.

It is evident that the tenacity and also the extension to break of normal-breaking fibers are much higher than are the corresponding values for weak-point breakage and higher than for breakage at the thinnest part of the fiber. $\bar{T}_{NT} < \bar{T}_{ND}$ indicates that the linear density of the fiber is high, that is the D_{min} measured by SIFAN is larger than the real value. In the weak-point breakage, as illustrated in Table II, $\bar{T}_{WWUD} < \bar{T}_{WD}$ and $\bar{\varepsilon}_{WWUD} < \bar{\varepsilon}_{WD}$ imply that the weakest link of wool fibers does not occur at the thinnest section but rather at the thick part, although there does exist some weak links at thin parts of the fiber.

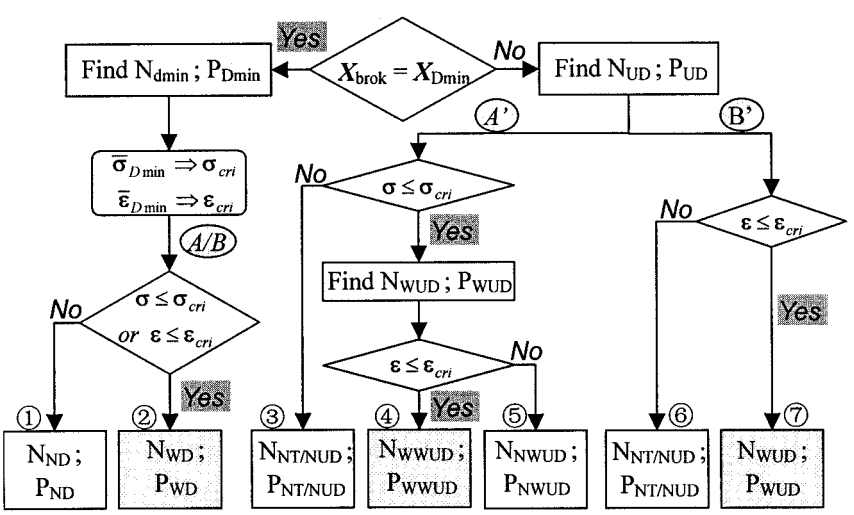

Figure 8 Schematic diagram for the identification of the fiber-breaking forms, where the subscriptions, *N* and *W*, *D* and *UD*, and *T*, represent the normal and the weak-point breakage, respectively, broken at and not at D_{min}, and broken at the true thinnest section, respectively.

TABLE II
Identification Criteria and Percentage of Various Fiber-breakage Forms

	Method											
	OM + XQ (SH80s)						SIFAN (SH80s)					
	Parameter											
	N^{σ}	P^{σ} (%)	T (cN/tex)	N^{ε}	P^{ε} (%)	ε (%)	N^{σ}	P^{σ} (%)	T (cN/tex)	N^{ε}	P^{ϵ}(%)	ε (%)
Total	342	100	20.2	342	100	36.6	254	100	20.3	254	100	34.7
D_{min}	203	59.4	21.5	203	59.4	35.3	123	48.4	21.8	123	48.4	33.1
WD	92	26.9	18.1	72	21.1	21.9	64	25.2	18.4	49	19.3	21.4
ND	111	32.5	25.2	131	38.3	42.4	59	23.2	25.4	74	29.1	40.9
UD_{min}	139	40.6	17.9	139	40.6	36.9	131	51.6	18.9	131	51.6	36.2
WUD	109	31.9	17.3	65	19.0	26.7	116	45.7	18.3	47	18.5	25.7
WWUD	50	14.6	15.9	—	—	—	45	17.7	16.9	—	—	—
NWUD	59	17.3	19.0	—	—	—	71	28.0	19.3	—	—	—
NT/NUD	30	8.8	22.6	74	21.6	44.9	15	5.9	23.0	84	33.1	42.1
W (weak)	142	41.5	17.4	137	40.1	24.3	109	42.9	17.8	96	37.8	23.5
N (normal)	200	58.5	22.9	205	59.9	43.4	145	57.1	22.1	158	62.2	41.5
Th (thinner)	292	85.4	21.1	277	81.0	37.8	209	82.3	21.0	207	81.5	36.8

CONCLUSIONS

The most important parameters measured by SIFAN are D_{min} and the ratio of D_{min}/D_{ave}. But D_{max} is frequently not a real value for the measured fiber due to the effect of the dust and nonfiber attachments so that the protubation peaks or pulses appearing on fiber profile curves should be removed to obtain a correct D_{ave}. The experimental parameters, such as the gauge length, fiber twist, and noncircular cross section and pretension, should also be considered in the SIFAN tests. Although there are many manual operations for the OM + XQ technique, it is relatively efficient to characterize the tensile behavior of fiber weak points.

The two forms of fiber weakpoints, that is, the thinnest part and the outer-structural weak point, were observed and described. The tensile and morphological characteristics of the structural weak points were defined. The probability of fiber breakage at D_{min} was evaluated in the range from 40 to 52%. The theory and criteria for weak-point identification based on fiber tensile curves were derived. The percentage of weak-point breakage and the difference of tensile properties between the weak-point breakage and the universal mean are important parameters required to evaluate wool quality in practice. According to the experimental results, the probabilities of weak-point, normal, and thinnest-part breakage can be evaluated by the new approach and approximate to 40, 60, and slightly more than 80%, respectively.

References

1. IWTO-8-66(E), IWTO, IWS; Raw Wool Service; Ilkley, England, 1966.
2. ASTM Standards, D 1282–96; Annual Book of ASTM Standards, 1998; Vol. 07.01.
3. Baxter, B. P.; Brims, M. A.; Taylor, T. B. In proceedings of the IWTO Technical Committee, Dec. 1991; Report No. 8.
4. Maher, A. P.; Daly, J. S. J Text Inst 1998, 89, 133–141.
5. IWTO Test Method 12; IWTO-12–93 (E).
6. Peterson, A. D.; Brims, A.; Brims, M. A.; Gherardi, S. D. J TextInst 1998, 89 (Part I), 441–448.
7. Baxter, B. P.; Brims, M. A.; Taylor, T. B. 1992. J Text Inst 1992, 83, 507–526.
8. Peterson, A. D.; Brims, A.; Brims, M. A.; Gherardi, S. D. Proc Aust Soc Anim Prod 1996, 21, 390.
9. Maher, A. P.; Daly, J. S. J Text Inst 1998, 89, (Part I), 133–141.
10. Anderson, L.; Cox, D. R. J Text Inst. 1950, 41, T481–491.
11. Woods, J. L.; Orwin, D. F.; Nelson, W. G. In Proceedings of the 8th International Wool Textile Research Conference, Christchurch, 1990, Vol. 1, pp 1557–568.
12. Hunter, L.; Leeuwner, W.; Smuts, S.; Strydom, M. A. SAWTRI Technical Report, No. 514, 1983.
13. Zimmermann, M.; Hocker, H. Text Res J 1996, 66, 657–660.
14. Orwin, D. F. G.; Woods, J. L.; Elliott, K. H. In Proceedings of the 6th International Wool Textile Research Conference, Pretoria, 1980; Vol. 2, pp 193–205.
15. Orwin, D. F. G.; Woods, J. L.; Gourdie, R. G. In Proceedings of the 7th International Wool Textile Research Conference, Tokyo, 1985, Vol. 1, pp 194–203.
16. Thorsen, W. J. Text Res J 1958, 28, 185–197.
17. Hepworth, A.; Buckley, T.; Sikorski, J. J Sci Instrum (J Phys E) Series 2 1969, 2, 789–796.
18. Hearle, J. W. S.; Jariwala, B. C.; Konopasek, L.; Lomas, B. In Proceedings of the 5th International Wool Textile Research Conference, Achen, 1975; Vol. II, pp 370–379.
19. Bandyopadhyay, S. 1984. In Symposium on Deformation, Failure and Strengthening of Polymers, Monash University, Australia, 1984; pp. 1–10.
20. Yang, X.; Sun, W.; Yan, H. J China Text Univ (Chin Ed) 1988, 14, 9–17.
21. Gharehaghaji, A. A.; Johnson, N. A. G.; Wang, X. J Text Inst 1999, 90 (Part I), 1–22.
22. Gharehaghaji, A. A.; Johnson, N. A. G.; Wang, X. J Text Inst 1999, 90 (Part I), 23–34.
23. Peirce, F. T. J Text Inst 1926, 17, T355–368.
24. Li, R.; Yan, W.; Shi, D. 1996. J China Text Univ (Chin Ed) 1996, 22(3), 1–4.